

See discussions, stats, and author profiles for this publication at: <https://www.researchgate.net/publication/23967686>

Functional Magnetic Resonance Imaging in Prostate Cancer

Article in *European Urology* · February 2009

Impact Factor: 13.94 · DOI: 10.1016/j.eururo.2009.01.027 · Source: PubMed

CITATIONS

87

READS

42

9 authors, including:



Amita Shukla-Dave

Memorial Sloan-Kettering Cancer Center

78 PUBLICATIONS 2,372 CITATIONS

SEE PROFILE



Anders Bjartell

Lund University

306 PUBLICATIONS 6,488 CITATIONS

SEE PROFILE



Alessandro Sciarra

Sapienza University of Rome

188 PUBLICATIONS 2,480 CITATIONS

SEE PROFILE



Anno Graser

Ludwig-Maximilians-University of Munich

157 PUBLICATIONS 2,197 CITATIONS

SEE PROFILE



Collaborative Review – Prostate Cancer

Functional Magnetic Resonance Imaging in Prostate Cancer

Michael Seitz^{a,*}, Amita Shukla-Dave^b, Anders Bjartell^c, Karim Touijer^d,
Alessandro Sciarra^e, Patrick J. Bastian^a, Christian Stief^a, Hedvig Hricak^f, Anno Graser^g

^aDepartment of Urology, University of Munich – Grosshadern Campus, Munich, Germany

^bDepartments of Radiology and Medical Physics, Memorial Sloan-Kettering Cancer Center, New York, NY, USA

^cDepartment of Urology, University Hospital Malmö, Lund University, Malmö, Sweden

^dDepartment of Surgery, Memorial Sloan-Kettering Cancer Center, New York, NY, USA

^eDepartment of Urology “U. Bracci,” University of Rome “Sapienza,” Rome, Italy

^fDepartment of Radiology, Memorial Sloan-Kettering Cancer Center, New York, NY, USA

^gDepartment of Radiology, University of Munich – Grosshadern Campus, Munich, Germany

Article info

Article history:

Accepted January 13, 2009

Published online ahead of
print on January 21, 2009

Keywords:

Functional MRI
Magnetic resonance
spectroscopy
Diffusion-weighted MRI
Dynamic contrast-enhanced
MRI
Prostate
Prostate cancer
Metabolic imaging
3 Tesla
1.5 Tesla
Active surveillance

Abstract

Context: Magnetic resonance imaging (MRI) combined with magnetic resonance spectroscopy imaging (MRSI), dynamic contrast-enhanced MRI, and diffusion-weighted MRI emerged as promising tests in the diagnosis of prostate cancer, and they show encouraging results.

Objective: This review emphasizes different functional MRI techniques in the diagnosis of prostate cancer and includes information about their clinical value and usefulness.

Evidence acquisition: The authors searched the Medline, Embase, and Cochrane Library databases. There were no language restrictions. The last search was performed in October 2008.

Evidence synthesis: The combination of conventional MRI with functional MRI techniques is more reliable for differentiating benign and malignant prostate tissues than any other diagnostic procedure. At present, no guideline is available that outlines which technique is best in a specific clinical situation. It also remains uncertain whether improved spatial resolution and signal-to-noise ratio of 3-T MRI will improve diagnostic performance.

Conclusions: A limited number of small studies suggest that functional MRI may improve the diagnosis and staging of prostate cancer. This finding needs further confirmation in larger studies, and cost-effectiveness needs to be established.

© 2009 European Association of Urology. Published by Elsevier B.V. All rights reserved.

* Corresponding author. Department of Urology, University of Munich – Grosshadern Campus, Marchioninstr. 15, 81377 Munich, Germany.
E-mail address: Michael.seitz@med.lmu.de (M. Seitz).

1. Introduction

Despite advances in prostate cancer (PCa) detection and treatment, the disease continues to represent an enormous healthcare burden. Among men in the European Union, PCa accounts for approximately 11% of all cancers and 9% of all cancer deaths [1].

The diagnosis of PCa is based on a combination of digital rectal examination (DRE), serum prostate-specific antigen (PSA) testing, and transrectal ultrasound (TRUS)-guided biopsy. In prostate cancer diagnosis or staging, neither computed tomography (CT) nor magnetic resonance imaging (MRI) are routinely recommended by European Association of Urology (EAU) guidelines. Since the gold standard for lymph node staging is still pelvic lymphadenectomy, cross-sectional imaging is only recommended in patients at high risk for lymphnode metastasis. Bone scan is the standard technique in patients at high risk for bone metastases [2,3].

Although MRI plays a limited role in published guidelines, it is increasingly gaining recognition as an important tool for the detection, localization, and staging of primary and recurrent PCa, permitting improved treatment selection and planning. Because the development of prostate cancer is associated with changes in metabolism, diffusion, and blood flow, functional magnetic resonance (MR) imaging techniques can aid in the detection and evaluation the disease.

The aim of this article is to review the current clinical status of advanced MRI techniques for the detection, staging, and follow-up of PCa, paying special attention to the needs of clinicians. All techniques described in this article are available and are clinically used at both 1.5-T and 3-T magnetic field strengths; therefore, MR-related technical issues will not be discussed.

2. Evidence acquisition

The authors searched the Medline, Embase, and Cochrane Library databases. There were no language restrictions. The last search was performed in October 2008.

3. Evidence synthesis

3.1. Magnetic resonance imaging of prostatic zonal anatomy

The normal anatomy of the prostate consists of four anatomic regions, first described by McNeal in

1981 [4]. In relation to these regions, the prostatic urethra provides a central anatomic reference point [1]. The peripheral zone (p-zone) constitutes >70% of the glandular prostate in younger men. The majority of all carcinomas arise here [2]. The central zone (c-zone) constitutes 25% of the glandular prostate. Marked histologic differences between c-zone and p-zone suggest important biologic differences. The small transitional zone (t-zone) and several periurethral ducts are the exclusive site of origin of benign prostatic hyperplasia (BPH) [4]. The anterior fibromuscular stroma forms the entire anterior surface of the prostate as a thick, nonglandular apron, covering the anterior surface of the three glandular regions. It is inseparably fused with the glandular prostate [4–6]. T2-weighted MRI is best suited to visualize the zonal anatomy of the prostate [4].

3.2. Advanced and functional magnetic resonance imaging techniques

Since the mid-1980s, intense research has focused on complementary techniques to improve the detection and staging of PCa. While proton magnetic resonance spectroscopic imaging (MRSI) can provide metabolic information, diffusion-weighted MRI (DW-MRI) allows in vivo measurement of diffusion coefficients of biological tissues, and dynamic contrast-enhanced MRI (DCE-MRI) enables noninvasive visualization of tissue vascularity.

3.2.1. Magnetic resonance spectroscopic imaging

In MRSI, a three-dimensional (3D) data set of the prostate is acquired, with volume elements (voxels) ranging from 0.24 cm³ to 0.34 cm³ in size [7,8]. This technique produces an array of MR spectra showing the relative concentrations of metabolites within voxels. MRI is followed by MRSI. The metabolic data from MRSI are superimposed onto MR images to help identify and localize PCa [9–11] (Figs. 1–5).

MRSI sequences suppress signal contributions from water and fat and emphasize contributions from metabolites that are characteristic for prostatic tissue and PCa. The metabolites measured by in vivo MRSI are citrate, creatine, choline, and polyamines. PCa is identified on MRSI by an increased ratio of choline plus polyamines plus creatine to citrate [12,13]. Today, different postprocessing software packages for spectroscopy are commercially available.

3.2.2. Diffusion-weighted magnetic resonance imaging

DW-MRI yields qualitative and quantitative information reflecting tissue cellularity and cell membrane integrity and thus complements morphologic in

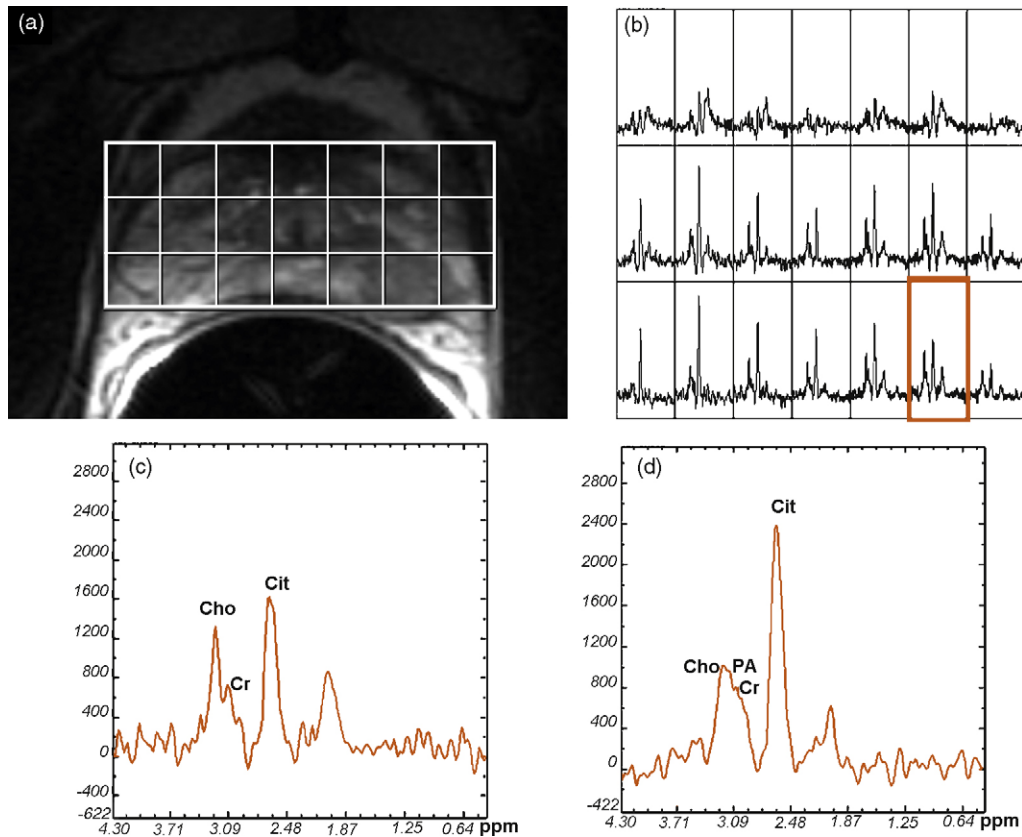


Fig. 1 – Magnetic resonance imaging (MRI) and magnetic resonance spectroscopic imaging (MRSI) data from a 46-yr-old patient with prostate cancer (clinical stage T2a, biopsy Gleason score 6, and prostate-specific antigen level of 4.2 ng/ml): (a) MRSI grid superimposed on transverse T2-weighted MRI; (b) low signal intensity in the left peripheral zone MRSI grid showing all spectra with voxel suspicious for cancer (outlined in bold black line); (c) spectrum of the voxel suspicious for cancer in the peripheral zone showing creatine (Cr), reduced citrate (Cit), elevated choline (Cho), and polyamines (PA) undetectable; (d) spectrum of a voxel from healthy peripheral zone tissue showing Cr, high Cit, equal PA, and Cho.

information obtained with conventional MRI. The motion of water molecules in extra- and intracellular spaces contributes to the net water displacement measured by DW-MRI. The degree of H₂O diffusion in biologic tissue is inversely correlated to the tissue cellularity and the integrity of cell membranes [14–17]. Generally, the motion of water molecules is more restricted in tissues with a high cellular density and intact cell membranes (eg, tumor tissue). The displacement of a single water molecule that occurs during a diffusion measurement is estimated to be approximately 8 μm. By comparison, the size of cells in the human body measure about 10 μm [18]. Qualitative (visual) assessment of relative tissue signal attenuation at DW-MRI is used for tumor detection and tumor characterization, while quantitative analysis of DW-MRI is achieved by calculation of the apparent diffusion coefficient (ADC). The ADC is calculated for each pixel of the image and is displayed as a parametric map (ADC map) [19]. In summary,

DW-MRI derives its image contrast from differences in the motion of water molecules between tissues. These images can be acquired quickly without the administration of exogenous contrast medium.

3.2.3. Dynamic contrast-enhanced magnetic resonance imaging

DCE-MRI is based on repetitive acquisition of sequential images during the passage of a contrast agent within a tissue of interest. It has long been known that an abnormal vasculature is an integral feature of tumors [20,21]. Techniques based on the assessment of neoangiogenesis, therefore, can only detect those tumors in which the angiogenic pathway has been turned on [20]. A number of features of tumor vascularity are characteristic of malignancy such as chaotic structure, arteriovenous shunting, high permeability, and areas of hemorrhage [22]. Furthermore, because the amount of interstitial space is greater in cancerous tissue than in normal tissue, there is a larger difference in contrast

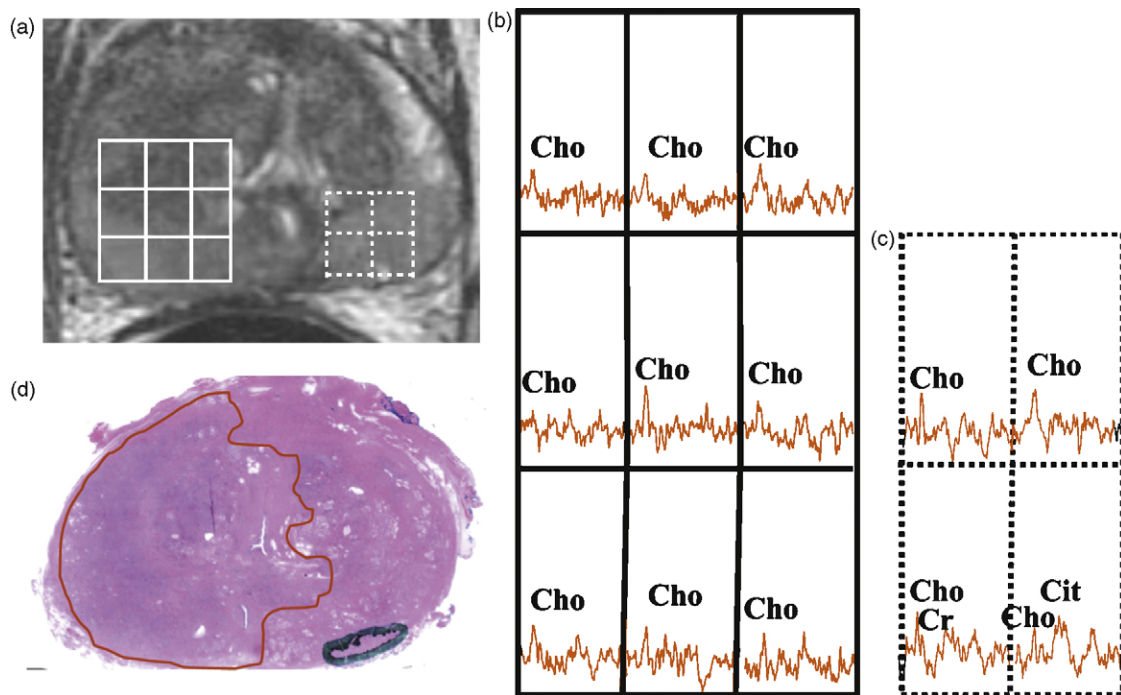


Fig. 2 – Magnetic resonance imaging (MRI), magnetic resonance spectroscopic imaging (MRSI), and pathologic data from a 57-yr-old patient with prostate cancer (clinical stage T1c, Gleason score of 6, and prostate-specific antigen level of 4.0 ng/ml). This patient had a clinical history of chronic prostatitis, and histopathologic findings confirmed severe chronic prostatitis and focal cancer. (a) Transverse T2-weighted MRI shows two regions of interest, one marked with solid lines and the other marked with dashed lines; regions of interest exhibit abnormal diffuse low signal intensity. (b) MRSI voxels marked with solid lines in (a) have a magnetic resonance (MR) spectral pattern of elevated choline and no citrate; these findings mimic those of cancer. (c) Voxels marked with a dashed line have an MR spectral pattern consistent with cancer. (d) Step-section pathologic map corresponds to MRI in (a), with chronic prostatitis marked with a thin line in the right half of the gland and cancer marked with a thick line in the left peripheral zone. Spectral findings at MRSI resulted in overestimation of voxels with a cancer-like pattern and caused false-positive findings. Adapted with permission from the Radiological Society of North America [86].

material concentration between the plasma and the interstitium [23,24]. MRI sequences have been designed that are sensitive to tissue perfusion and blood volume (so-called T2* methods) or microvessel perfusion, permeability, and extracellular leakage space (so-called T1 methods). At present, there are only limited data on T2*-weighted MRI and PCa in the literature and most authors have been focusing on T1-weighted DCE-MRI [20,21].

DCE-MRI enables the visualization of lesion vasculature and permeability. DCE-MRI may allow noninvasive characterization of PCa and, therefore, may play a role in tumor detection and therapy monitoring.

3.3. Diagnostic accuracy of magnetic resonance imaging techniques at 1.5 T

3.3.1. Tumor detection and localization

3.3.1.1. *Magnetic resonance imaging.* Reviewing the literature, Engelbrecht et al [25], examined factors

influencing the heterogeneous reported staging performance of MRI. Their results suggest that the use of fast spin echo, an endorectal coil, and multiple imaging planes improve staging performance. Additionally, the group showed that in distinguishing between PCa stages T2 and T3, MRI has a combined sensitivity and specificity of 71%. In contrast, a cohort study [26] on >300 consecutive patients with biopsy-proven PCa compared preoperative MRI findings to clinical data in the prediction of extracapsular extension (ECE). In the evaluation of ECE, endorectal MRI findings had sensitivity, specificity, positive predictive value (PPV), and negative predictive value (NPV) of 42.2%, 95.4%, 74.5%, and 83.8%, respectively. In a multivariate analysis to predict ECE, the area under the receiver operating characteristic (ROC) curve (0.838) was greater for the model with clinical variables and endorectal MRI findings than that for the model with clinical variables alone (0.772; $p = 0.022$). In a study of >600 patients, the same

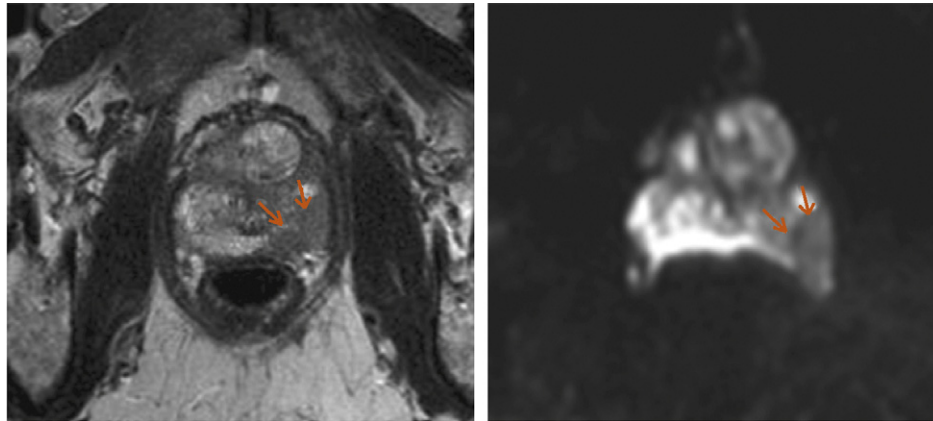


Fig. 3 – A 3-T magnetic resonance image (MRI) (left) and diffusion-weighted MRI (right) in a 67-yr-old male with stage T2b prostate cancer in the left midgland. T2-weighted axial image acquired at 3 T without endorectal coil shows confluent area of hypointense signal in the left peripheral zone (arrows). The corresponding diffusion-weighted image (b-value: 500) shows restricted diffusion in the same area, most consistent with prostate cancer. Histopathology showed a tumor Gleason score of 6.

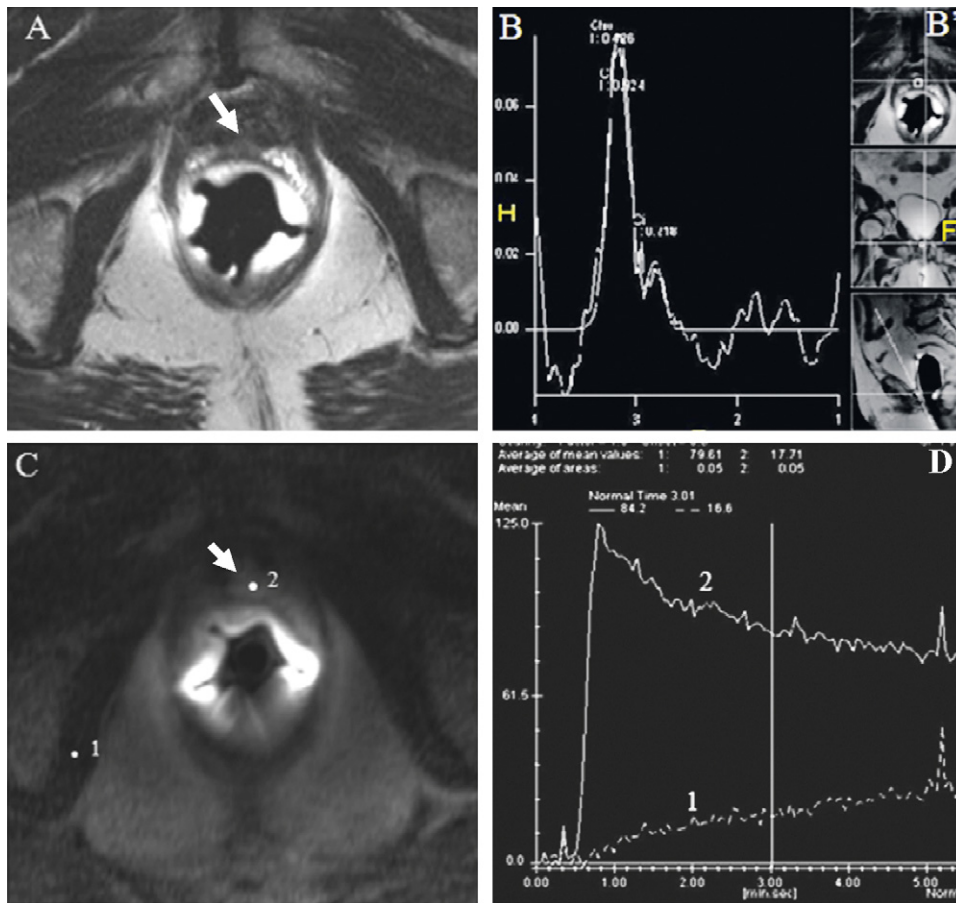


Fig. 4 – T2-weighted magnetic resonance imaging (MRI) and dynamic contrast-enhanced MRI (DCE-MRI) in a patient with suspected local recurrence after radical prostatectomy: (A) T2-weighted, 1.5-T MRI without endoscopic retrograde cholangiography (ERC) shows focal hypointense signal at the site of anastomosis after radical prostatectomy; (B) magnetic resonance spectroscopic imaging (MRSI) confirms the presence of tumor tissue by showing an abnormal spectrum (high choline and creatine peak, low citrate); additionally, (C) DCE-MRI displays hyperperfusion (curve 2) of tumor tissue in comparison to (D) obturator muscle (curve 1).

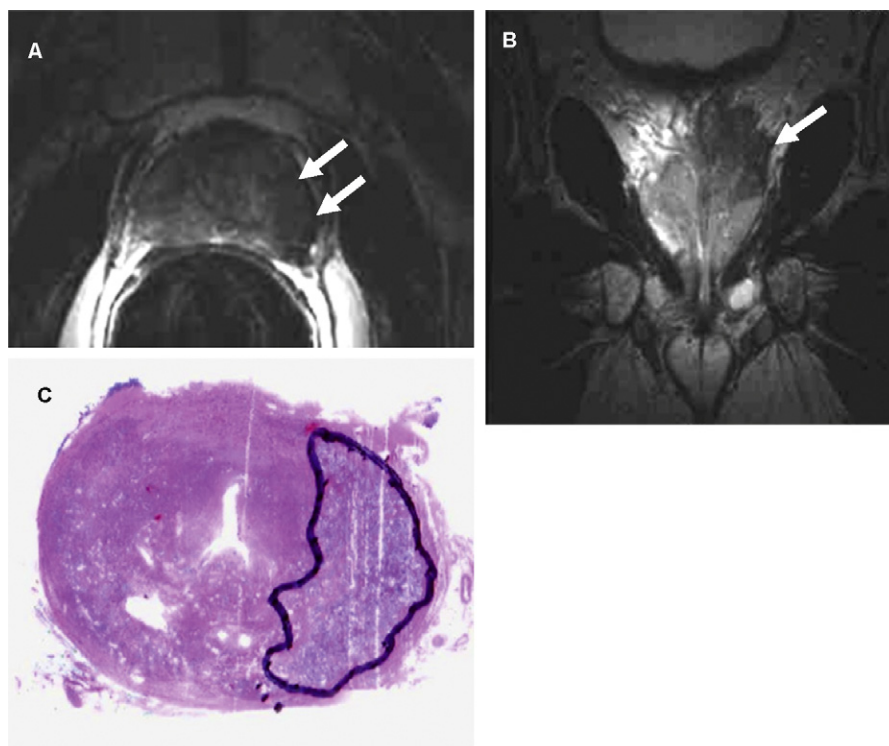


Fig. 5 – Endoscopic retrograde cholangiography (ERC) magnetic resonance imaging (MRI) in a patient treated with external beam radiotherapy and a current serum prostate-specific antigen (PSA) level of 4.5 ng/ml. (A) T2-weighted MRI shows uniform hypointense signal throughout the gland, a finding that is characteristic after radiation therapy; markedly decreased signal is seen in the left peripheral zone (arrows). (B) The coronal T2-weighted image shows that the tumor invades the left seminal vesicle. (C) The patient subsequently underwent salvage prostatectomy, and whole mount histopathology confirmed presence of cancer in left peripheral zone.

group confirmed that MRI contributed an incremental value to the preoperative Partin tables (2001 version) in the prediction of organ-confined PCa. The area under the ROC curve for the preoperative staging nomogram was 0.80, while the area under the ROC curve for the combination of nomogram and MRI findings was 0.88 ($p < 0.01$) [27]. Similarly, MRI was found to add significant incremental value to the standard clinical nomogram for predicting seminal vesicle invasion (SVI) [28]. A wide range of accuracy levels have been reported for MRI in the detection of ECE (from 54% to 83%) [29–32] and SVI (from 81% to 93%) [33–35].

In terms of discrimination between benign and malignant tissue (detection accuracy) in men with suspected PCa and elevated PSA levels, most studies use prostate needle-biopsy pathology as a (poor) reference standard to rule out or confirm malignancy. In seven studies with mean patient serum PSA levels ranging from 6.55 ng/ml to 19.4 ng/ml, ranges for the sensitivity, specificity, PPV, NPV, and accuracy of MRI were 41.2–100%, 50–97%, 34.8–77.8%, 63–100%, and 64–75.9%, respectively [36–42].

False-positive rates as low as 6% and as high as 35% have been reported [43,44] and have been attributed to postbiopsy hemorrhage, prostatitis, and glandular or fibrous hyperplasia foci.

3.3.1.2. Advanced magnetic resonance imaging techniques. The first advanced MRI technique that was evaluated in larger studies is MR spectroscopy imaging (MRSI). Due to its ability to show abnormalities in prostate metabolism, MRSI adds incremental information to morphological MR images. Scheidler et al [9] demonstrated that the addition of 3D MRSI to MRI improves PCa detection and localization on a per-sextant basis, increasing the sensitivity and specificity; for locations in the p-zone, PPV and NPV were 89–92% and 74–82%, respectively. The same group proposed the use of 3D MRSI to improve accuracy and reproducibility in the prediction of ECE [45]. When compared with nomograms (Partin tables, 2001 version) alone, the combination of MRI/MRSI and nomograms performed significantly better in predicting organ-confined disease and SVI. Accuracy in the prediction of organ-confined PCa with MRI was

higher when MRSI was used, but the difference was not significant [27,28]. Recent retrospective studies [11,12,46–48] in patients with PCa confirmed at surgical pathology found that combined MRI/MRSI had sensitivity of 42–93%, specificity of 81–89.3%, accuracy of 74–85%, NPV of 50–86%, and PPV of 81–93%, respectively, in staging PCa. When combined MRI/MRSI was investigated for tumor localization on a per-sextant basis, MRI and 3D MRSI were each more sensitive (67% and 76%, compared with 50%, respectively), but less specific (69% and 57%, compared with 82%, respectively) than sextant prostate biopsy. MRI and combined 3D MRSI have also been shown to be superior to sextant biopsy, with the largest increase in diagnostic accuracy at the apex of the prostate, which is difficult to reach by biopsy [47]. One study found that when cancer was detected on both MRI and MRSI, the combination of the two modalities had a PPV of 89–92% for prostate cancer in a sextant, while sensitivity and specificity were calculated to be 63% and 75%, respectively [9]. A recent prospective study in 39 patients with elevated PSA levels that used prostate biopsy as reference standard showed that combined MRI/MRSI reached a 79% accuracy in the localization of PCa [49], which is in agreement with a single-institutional study on 42 patients with a reported accuracy of 74.2% for tumor detection in the prostate [50].

While MRSI depicts intraprostatic metabolism, DW-MRI is employed to assess the degree of water diffusivity within a given volume of interest. Generally, the motion of water molecules is restricted in areas of PCa, which leads to decreased signal intensity in both diffusion-weighted and ADC images. In an early clinical retrospective single-institutional study comparing MRI to combined MRI and DW-MRI in 124 consecutive patients with clinically suspected PCa (mean PSA level: 21.8 ng/ml), the sensitivity, specificity, PPV, and NPV of combined MRI/DW-MRI for prostate cancer were reported to be 86%, 84%, 90%, and 79%, respectively [51]. Another prospective, single-institution study of 33 patients showed that ADC values of malignant prostate tissue were significantly lower than in benign tissue. In this study, DW-MRI had a reported sensitivity of 86.7% and specificity of 72.2% for identifying malignant p-zone lesions [52]. In a prospective study of 56 patients (PSA level between 2.3 ng/ml and 46 ng/ml), Morgan et al showed improved sensitivity (73.2% for combined MRI/DW-MRI vs 50% for MRI alone) for an experienced reader in PCa detection. Specificity, accuracy, PPV, and NPV also improved from 79.6% to 80.8%, 66.6% to 77.5%, 65.7% to 74.8%, and 67.1% to 79.5%, respectively [53]. Recently, a study using surgical pathology

as the reference standard demonstrated that the addition of DW-MRI to MRI significantly increased the detection rate of PCa in the t-zone. This study also revealed a relationship between histologic grade expressed by Gleason score and ADC values [54]. A recent study was the first to confirm on whole-mount, step-section pathology that there was a significant difference in ADC between BPH and PCa; this study also showed a significant overlap in ADC values of cancer and normal tissue, suggesting that not absolute ADC values, but rather relative differences in ADC values in each individual patient are important [55].

While DW-MRI techniques focus on motion of water molecules in different tissues, DCE-MRI aims at depiction of vascularity. Generally, malignant tumors tend to enhance more strongly and avidly than healthy prostate tissue, which leads to a more pronounced signal increase on T1-weighted, time-resolved imaging. Clinical experiences with the technique were first reported in the mid-1990s and many studies have found functional DCE-MRI to be superior to morphological T2-weighted MRI alone. In 1997 Jager et al [56] reported that the sensitivity and accuracy for DCE-MRI (73.5% and 77.5%, respectively) were higher than for MRI alone (57.5% and 72%, respectively), and that specificities were equivalent for the two techniques (80.5% for MRI vs 81% for DCE-MRI). Several studies on DCE-MRI that used surgical pathology as the reference standard have reported sensitivity, specificity, and accuracy levels ranging from 69% to 95%, from 80% to 96.2%, and from 77.5% to 92%, respectively [56–61]. In a prospective study of 34 patients using whole-mount histopathology as the reference standard, Fütterer et al [61] found that for the localization of tumors with volumes of ≥ 0.5 cm³, interpretation of T1-weighted DCE-MRI in conjunction with T2-weighted MRI led to an increase in sensitivity from 69% to 95%, while specificity (80–96%) and accuracy (81–93%) also increased. For the assessment of ECE, the diagnostic accuracy of combined MRI and DCE-MRI was 95–96%. Sensitivity, specificity, PPV, and NPV were 82–91%, 95%, 90–91%, 91–95%, respectively. With combined MRI and DCE-MRI, understaging occurred in 3–9%, and overstaging occurred in 3–6% of patients [62]. Recently, Ren et al investigated the correlation between enhancement rate, expression levels of vascular endothelial growth factor (VEGF), and microvascular density (MVD) in both prostate cancer and BPH; the group reported that VEGF expression and MVD were significantly higher in PCa than in BPH. They also found a positive correlation between the degree of enhancement, expression levels of VEGF, and MVD, and therefore

concluded that DCE-MRI has the potential to depict and monitor tumor angiogenesis [63].

In an attempt to improve PCa detection, several study groups have investigated combinations of advanced MR techniques in order to further improve diagnostic accuracy in the localization of PCa. In a prospective study, 83 consecutive male patients with clinical suspicion of PCa underwent T2-weighted MRI, DCE-MRI, and DW-MRI before biopsy. In ROC analyses the A_z -values were 0.711, 0.905, and 0.966 for T2-weighted MRI alone, T2-weighted MRI plus DW-MRI, and T2-weighted MRI plus DW-MRI and DCE-MRI, respectively [40]. In a different retrospective single-institutional study, another group investigated 42 patients with elevated PSA levels; A_z -values were 0.848, 0.860, and 0.961 for T2-weighted MRI, DW-MRI, and MRSI, respectively. When all three techniques were used in unison, the A_z -value increased to 0.978, which led to the conclusion that PCa may be more effectively diagnosed by a combination of the three techniques than by using any of them alone [41]. Other studies showed similar results with improved PCa detection for combined MR protocols [50,64,65].

In summary, advanced functional imaging techniques significantly increase the sensitivity of MRI in the detection and staging of prostate cancer. MRSI, DW-MRI, and DCE-MRI all deliver additional information to morphologic changes depicted on T2-weighted MR images. It is important to carefully tailor MRI examination protocols to individual patient clinical history; if applied to appropriately selected patients, each of the three techniques will help to better characterize, stage, and grade potential malignancy of the prostate.

3.3.2. Clinically suspected prostate cancer after previous negative biopsy

One of the most challenging clinical settings concerns patients with persistent elevation of serum PSA levels and previous negative transrectal biopsies of the prostate. Several recent publications on MRI techniques focus on this clinical setting. In this patient cohort, an ideal diagnostic test would provide a high NPV in order to minimize unnecessary repeat prostate biopsies. In a prospective analysis, Beyersdorff et al found a sensitivity of 83% and a PPV of 50% for detection of PCa at MRI (DRE: 33% and 67%; TRUS: 33% and 57%). At site-by-site analysis, MRI results did not correlate significantly with individual biopsy site findings [66]. Another study assessed the value of endorectal MRI in the prediction of negative biopsies and compared it to PSA levels and DRE findings. Some 92 patients with elevated PSA levels (>4 ng/ml) and/

or abnormal DRE findings underwent one to five sets of TRUS-guided prostate biopsies after MRI. The combination of MRI with DRE and PSA had the highest accuracy (83%) in PCa detection, significantly higher than that of DRE or PSA alone (70%). The probability of a positive biopsy result in patients PSA values between 5 mg/ml and 15 ng/ml and negative findings on DRE and MRI was 5–10% at first and second biopsies but decreased progressively to $<3\%$ at the fifth biopsy. The conclusion of this study was that in patients with elevated serum PSA levels and/or abnormal DREs who have undergone two negative biopsy sessions, a negative endorectal MRI examination may be sufficient to avoid subsequent biopsies [67].

In each of 24 patients with at least one negative prostate biopsy session, Yuen et al [68] performed 10 random biopsies and up to 4 targeted biopsies that aimed at areas positive for PCa at MRI and/or MRSI. Prostate cancer was detected at biopsy in seven patients; in two of these seven patients, cancer would have been missed if TRUS-guided biopsy had not been directed at the abnormal areas detected by MRI and/or MRSI. Combined MRI/MRSI detected prostate cancer on a per-patient basis with an accuracy of 79.2% and with sensitivity, specificity, PPV, and NPV of 100%, 70.6%, 58.3%, and 100%, respectively. In another study, combined MRI/MRSI was performed in 42 patients with an average of two previously negative prostate biopsies and an average PSA level of 12 ng/ml (range: 3.9–35 ng/ml). Following imaging, each patient had 10 targeted biopsies. Among 15 patients with biopsy results positive for PCa, tumor locations were identical for biopsies and combined MRI/MRSI of the prostate in nine cases, and identical for biopsies and MRSI alone in another five cases. MRI/MRSI had sensitivity of 73.3% and specificity, PPV, NPV, and accuracy of 96.3%, 91.6%, 86.6% and 88%, respectively [69]. Accordingly, targeted biopsies may improve the diagnostic yield to a greater degree than an increased number of biopsies. The first study using DCE-MRI before repeat biopsy showed rather disappointing results on 26 consecutive patients. Although endorectal MRI before TRUS guided prostate biopsy tended to detect a greater number of cancers, the difference was not statistically significant. With a NPV of 14% and 15% for T2-weighted MRI and DCE-MRI, respectively, combining the two techniques did not lead to better detection rates. When either T2-weighted MRI or DCE-MRI was positive; sensitivity and specificity were 40% and 66.4%, respectively [70].

In summary, MRI appears to be useful for ruling out cancer in patients at risk for PCa with previous

negative biopsies; in addition, there is evidence that the use of MRI to plan targeted biopsies may lead to the detection of cancers that would have been missed on systematic biopsies.

3.3.3. T2-weighted magnetic resonance imaging and complementary techniques in the setting of prostate specific antigen level relapse after definitive treatment

The key clinical consideration in evaluating patients with suspected recurrence is the differentiation between local and metastatic disease based on clinical parameters such as pathologic stage and tumor grade at the time of definitive treatment, PSA doubling time, time interval between surgery and PSA relapse, and nomograms. Patients with local recurrence following external beam radiation therapy (EBRT) may be considered to be good candidates for salvage prostatectomy, while patients with a PSA serum level of ≤ 1.5 ng/ml after radical prostatectomy are best treated by salvage radiation therapy [1]. CT and bone scan are of inferior diagnostic value in patients considered for salvage therapy, who typically have low PSA levels. Although nomograms help to statistically differentiate between local and distant relapse, the usefulness of nomograms is limited in an individual patient. Hence, imaging for the detection of local recurrence is of great importance. Conventional MRI and complementary functional MRI techniques have shown promise in the evaluation of the postsurgical pelvis.

3.3.3.1. *Magnetic resonance imaging of local recurrence after prostatectomy.* The value of endorectal coil MRI in detecting local recurrence after prostatectomy was shown by Silverman and Krebs [71]. In their study of 31 men with biopsy-proved local recurrence, 100% sensitivity and 100% specificity were achieved using unenhanced and contrast-enhanced sequences. Similarly, Sella et al reported a sensitivity of 95% and specificity of 100% in detecting local recurrence using unenhanced T1-weighted and T2-weighted sequences [72]. While all recurrences reported by Silverman and Krebs were located close to the site of anastomosis, Sella et al found only 29% of the recurrences in this location, while 40% were retrovesical. Retained seminal vesicles have been found on MRI in as many as 20% of patients after radical prostatectomy, and this common finding must be recognized so that it is not misinterpreted as a local recurrence [72]. In a recent report, after definitive treatment for PCa, 51 men underwent combined endorectal coil MRI and DCE-MRI before TRUS-guided biopsy of the prostatic fossa. While MRI alone achieved only an accuracy of 48%, combined MRI/DCE-MRI had an accuracy of 94% [73]. Only one

study evaluated the sensitivity and specificity of MRI/MRSI and DCE-MRI individually and in combination in the detection of PCa local recurrence after radical prostatectomy. Sciarra et al [74] performed an analysis in a cohort of 50 patients with biopsy-proven cancer recurrence (mean serum PSA level: 1.26 ng/ml) and in a second group of 20 patients with a reduction in PSA level $>50\%$ following radiation therapy (mean serum PSA level: 0.8 ng/ml). The sensitivity, specificity, PPV, and NPV of combined MRSI/DCE-MRI were 87%, 94%, 96%, and 79%, respectively, in group A and were 86%, 100%, 100% and 75%, respectively, in group B. ROC-analysis showed that MRSI performed less well in the postradiation group than in the postsurgery group, which may reflect the fact that the required voxel size for spectroscopic imaging is larger than that for DCE-MRI, an issue that may be especially relevant in small-volume disease.

3.3.3.2. *Magnetic resonance imaging of local recurrence after external beam radiation therapy.* Imaging is a great challenge in patients with increasing PSA levels after EBRT. To date, prostate biopsy is the exclusive method to confirm or rule out recurrence. Due to sampling errors a false-negative rate of 20% has been reported for biopsy [1]. The first study on nine patients that correlated MRI and MRSI after EBRT with histopathology compared sextant tumor localization by DRE, sextant biopsy, MRI, and MRSI. MRI, sextant biopsy, and DRE each had $>90\%$ specificity for sextant tumor localization; however, MRI had greater sensitivity (68%) than sextant biopsy (45%) and DRE (16%). MRSI had higher sensitivity (77%) but lower specificity (78%). Since metabolically altered benign tissue may be misinterpreted as tumor, the authors concluded that combined MRI/MRSI might be of limited benefit in evaluating patients with increasing PSA levels after EBRT [75]. In contrast, other authors suggested that MRSI but not MRI may be of value for the depiction of locally recurrent PCa after EBRT. In a study by Coakley et al that used biopsy findings as the reference standard, MRSI was significantly more accurate than MRI in detecting local recurrence of PCa. The presence of three or more suspicious voxels in a hemiprostate at MRSI had sensitivity and specificity of 89% and 82%, respectively for diagnosing local recurrence [76]. Sella et al retrospectively assessed the accuracy of endorectal MRI for depicting tumor, ECE, and SVI before salvage prostatectomy in patients with locally recurrent PCa after radiation therapy [72]. They found that areas under the ROC curve for two readers were 0.61 and 0.75 for the detection and localization of PCa, 0.76

and 0.87 for ECE, and 0.70 and 0.76 for SVI. Although MRI after EBRT and before salvage prostatectomy showed substantial interobserver variability, even between readers with similar experience, the authors suggested that the accuracy of endorectal MRI in tumor evaluation before salvage prostatectomy is similar to that of endorectal MRI in a pretreatment setting.

3.4. Advanced magnetic resonance imaging techniques in characterization of prostate cancer

Theoretically, advanced MRI techniques should be able to provide information about tumor aggressiveness (ie, Gleason score, because they assess metabolism, water diffusivity, and vascularity). In an attempt to determine whether metabolic information provided by MRSI could be used to predict the aggressiveness of PCa, Zakian et al [77] investigated 123 men prior to prostatectomy and found MRSI was more sensitive in patients with poorly differentiated neoplasms (Gleason scores $\geq 7b$). Tumors with a Gleason score of 6 that were not detected with MRSI had significantly smaller average diameters than those that were detected [78].

Using DW-MRI, DeSouza [52] demonstrated that water diffusion within prostate tumors was significantly different in patients with low-risk disease than in patients with intermediate or high-risk disease; they concluded that DW-MRI can potentially identify poorly differentiated tumors as these demonstrate earlier and faster enhancement [56]. Other studies did not confirm these findings [79–82]. Shukla-Dave et al [83] designed new nomogram models combining clinical variables and biopsy data with MRI and MRSI, and assessed their value in predicting the probability of insignificant ($<0.5\text{ cm}^3$) PCa. The most discriminating model combined the variables from the Kattan medium nomogram model (clinical stage T1c or T2a; primary and secondary biopsy Gleason grade 1–3 [score ≤ 6]; pretreatment PSA level of $<20\text{ ng/ml}$; $\leq 50\%$ of biopsy cores positive) with MRI/MRSI and had an area under the ROC curve of 0.854; it was significantly more accurate than the most accurate clinical model, which had an area under the curve (AUC) of 0.726.

In summary, advanced MRI may be beneficial in characterizing PCa and selecting appropriate treatment. Patients with clinically low-risk disease are faced with the particularly difficult decision of whether or not to undergo radical treatment. In the absence of other biomarkers, functional MRI may help address this problem, especially for patients who choose active surveillance, which currently

relies on PSA kinetics and the histology of prostate biopsy. However, PCa is histologically heterogeneous and is multifocal in most patients, and the biopsy Gleason score is subject to sampling error. It has been reported that the biopsy Gleason score is upgraded in as many as 54% of patients after radical prostatectomy [84]. Thus, a noninvasive technique that could be used to assess PCa aggressiveness and could accurately predict the pathologic Gleason score could make a substantial contribution to the decision-making process in patients with PCa.

4. Conclusions

The addition of functional MRI techniques to T2-weighted MRI can provide metabolic information, display altered cellularity, and aid in noninvasive characterization of tissue and tumor vascularity. This may improve PCa detection, localization, and primary staging. From a clinical point of view, there are three major concerns: (1) discrimination between cancer and benign processes in patients suspected to have PCa; (2) detection of PCa in patients with previous negative prostate biopsies and persistent elevation of serum PSA; and (3) local staging once PCa is diagnosed, which is of key importance to aid in treatment selection and planning (eg, nerve-sparing prostatectomy, wide-excision approach, EBRT, or brachytherapy). The combination of conventional MRI and functional MRI techniques is more reliable for differentiating and benign and malignant prostate tissues than any other diagnostic procedure and can help address these major concerns.

Another major concern in daily practice is how to address PSA-relapse after definitive treatment. In this setting, combined MRI/MRSI and DCE-MRI seem to be the diagnostic tools of choice. Although some authors favor choline-based positron emission tomography (PET) or CT scanning, MRI provides better spatial resolution and enables detection of recurrence in the low PSA range. Confirmation of local recurrence by imaging can play an important role in the decision-making process for patients with PSA relapse, since local recurrences following EBRT or prostatectomy may be treated by salvage radiation therapy or salvage prostatectomy, respectively. Despite rapid advances in imaging technologies, large randomized studies demonstrating the usefulness of different MR techniques have yet to be completed. Furthermore, no guidelines or reports are available outlining which technique is best in a specific clinical situation, and the clinician is left to utilize the technology available at his or her own

institution. It also remains uncertain whether improved spatial resolution and signal-to-noise ratio of a 3-T MRI will improve the diagnostic performance or will be beneficial in the imaging workup of patients with PCa.

We did not address the topic of MR-guided prostate biopsy (for more on this subject, readers are referred to an excellent review article by Pondman et al [85]), and we did not address the use of MRI techniques to assess treatment response (eg, changes caused by androgen deprivation therapy or radiation), as we felt that these approaches are rather academic and unlikely to influence the daily work of the urologist. In contrast, the correlation of functional MRI techniques with pathologic findings such as Gleason score and tumor volume to discriminate between significant and insignificant cancers should be of great interest, as it addresses the currently evolving field of approaching localized PCa conservatively. Active surveillance with regular PSA testing, serial DRE, and periodic repeat prostate biopsies have been proposed as an alternative to immediate treatment, with excellent long-term results. Functional MRI techniques may be incorporated in active surveillance programs to reduce repeat biopsies and biopsy sampling errors. As MRI technology continues to advance, MRI will become more and more accurate for diagnosing and staging PCa.

Author contributions: Michael Seitz had full access to all the data in the study and takes responsibility for the integrity of the data and the accuracy of the data analysis.

Study concept and design: Seitz, Hricak, Graser, Bjartell, Touijer, Stief.

Acquisition of data: Seitz, Hricak, Graser.

Analysis and interpretation of data: Seitz, Hricak, Graser.

Drafting of the manuscript: Seitz, Graser.

Critical revision of the manuscript for important intellectual content: Seitz, Hricak, Graser, Bjartell.

Statistical analysis: none.

Obtaining funding: none

Administrative, technical, or material support: Graser, Shukla-Dave, Sciarra, Bastian.

Supervision: Stief.

Other (specify): none.

Financial disclosures: I certify that all conflicts of interest, including specific financial interests and relationships and affiliations relevant to the subject matter or materials discussed in the manuscript (eg, employment/affiliation, grants or funding, consultancies, honoraria, stock ownership or options, expert testimony, royalties, or patents filed, received, or pending), are the following: none.

Funding/Support and role of the sponsor: none.

References

- [1] Heidenreich A, Aus G, Bolla M, et al. EAU guidelines on prostate cancer. *Eur Urol* 2008;53:68–80.
- [2] Ketelsen D, Röthke M, Aschoff P, et al. Detection of bone metastasis of prostate cancer—comparison of whole-body MRI and bone scintigraphy [in German]. *Rofo* 2008; 180:746–52.
- [3] Tuncel M, Souvatzoglou M, Herrmann K, et al. [(11)C]Choline positron emission tomography/computed tomography for staging and restaging of patients with advanced prostate cancer. *Nucl Med Biol* 2008;35:689–95.
- [4] McNeal JE. The zonal anatomy of the prostate. *Prostate* 1981;2:35–49.
- [5] McNeal JE. Normal histology of the prostate. *Am J Surg Pathol* 1988;12:619–33.
- [6] McNeal JE, Redwine EA, Freiha FS, Stamey TA. Zonal distribution of prostatic adenocarcinoma. Correlation with histologic pattern and direction of spread. *Am J Surg Pathol* 1988;12:897–906.
- [7] Hersh MR, Knapp EL, Choi J. Newer imaging modalities to assess tumor in the prostate. *Cancer Control* 2004;11: 353–7.
- [8] Heuck A, Scheidler J, Sommer B, Graser A, Muller-Lisse UG, Massmann J. MR imaging of prostate cancer [in German]. *Radiologe* 2003;43:464–73.
- [9] Scheidler J, Hricak H, Vigneron DB, et al. Prostate cancer: localization with three-dimensional proton MR spectroscopic imaging—clinicopathologic study. *Radiology* 1999; 213:473–80.
- [10] Kurhanewicz J, Vigneron DB, Hricak H, Narayan P, Carroll P, Nelson SJ. Three-dimensional H-1 MR spectroscopic imaging of the in situ human prostate with high (0.24–0.7 cm³) spatial resolution. *Radiology* 1996;198:795–805.
- [11] Mueller-Lisse UG, Vigneron DB, Hricak H, et al. Localized prostate cancer: effect of hormone deprivation therapy measured by using combined three-dimensional 1H MR spectroscopy and MR imaging: clinicopathologic case-controlled study. *Radiology* 2001;221:380–90.
- [12] Jung JA, Coakley FV, Vigneron DB, et al. Prostate depiction at endorectal MR spectroscopic imaging: investigation of a standardized evaluation system. *Radiology* 2004;233: 701–8.
- [13] Shukla-Dave A, Hricak H, Moskowitz C, et al. Detection of prostate cancer with MR spectroscopic imaging: an expanded paradigm incorporating polyamines. *Radiology* 2007;245:499–506.
- [14] Guo Y, Cai YQ, Cai ZL, et al. Differentiation of clinically benign and malignant breast lesions using diffusion-weighted imaging. *J Magn Reson Imaging* 2002;16:172–8.
- [15] Gauvain KM, McKinstry RC, Mukherjee P, et al. Evaluating pediatric brain tumor cellularity with diffusion-tensor imaging. *AJR Am J Roentgenol* 2001;177:449–54.
- [16] Sugahara T, Korogi Y, Kochi M, et al. Usefulness of diffusion-weighted MRI with echo-planar technique in the evaluation of cellularity in gliomas. *J Magn Reson Imaging* 1999;9:53–60.
- [17] Lang P, Wendland MF, Saeed M, et al. Osteogenic sarcoma: noninvasive in vivo assessment of tumor necrosis with

- diffusion-weighted MR imaging. *Radiology* 1998;206:227-35.
- [18] Sehy JV, Banks AA, Ackerman JJ, Neil JJ. Importance of intracellular water apparent diffusion to the measurement of membrane permeability. *Biophys J* 2002;83:2856-63.
- [19] Koh DM, Collins DJ. Diffusion-weighted MRI in the body: applications and challenges in oncology. *AJR Am J Roentgenol* 2007;188:1622-35.
- [20] Knopp MV, Giesel FL, Marcos H, von Tengg-Kobligk H, Choyke P. Dynamic contrast-enhanced magnetic resonance imaging in oncology. *Top Magn Reson Imaging* 2001;12:301-8.
- [21] Padhani AR, Husband JE. Dynamic contrast-enhanced MRI studies in oncology with an emphasis on quantification, validation, and human studies. *Clin Radiol* 2001;56:607-20.
- [22] Dvorak HF, Nagy JA, Feng D, Brown LF, Dvorak AM. Vascular permeability factor/vascular endothelial growth factor and the significance of microvascular hyperpermeability in angiogenesis. *Curr Top Microbiol Immunol* 1999;237:97-132.
- [23] Delorme S, Knopp MV. Noninvasive vascular imaging: assessing tumour vascularity. *Eur Radiol* 1998;8:517-27.
- [24] Yamashita Y, Baba T, Baba Y, et al. Dynamic contrast-enhanced MR imaging of uterine cervical cancer: pharmacokinetic analysis with histopathologic correlation and its importance in predicting the outcome of radiation therapy. *Radiology* 2000;216:803-9.
- [25] Engelbrecht MR, Jager GJ, Laheij RJ, Verbeek AL, van Lier HJ, Barentsz JO. Local staging of prostate cancer using magnetic resonance imaging: a meta-analysis. *Eur Radiol* 2002;12:2294-302.
- [26] Wang L, Mullerad M, Chen HN, et al. Prostate cancer: incremental value of endorectal MR imaging findings for prediction of extracapsular extension. *Radiology* 2004;232:133-9.
- [27] Wang L, Hricak H, Kattan MW, Chen HN, Scardino PT, Kuroiwa K. Prediction of organ-confined prostate cancer: incremental value of MR imaging and MR spectroscopic imaging to staging nomograms. *Radiology* 2006;238:597-603.
- [28] Wang L, Hricak H, Kattan MW, et al. Prediction of seminal vesicle invasion in prostate cancer: incremental value of adding endorectal MR imaging to the Kattan nomogram. *Radiology* 2007;242:182-8.
- [29] Beyersdorff D, Taymoorian K, Knosel T, et al. MRI of prostate cancer at 1.5 and 3.0 T: comparison of image quality in tumor detection and staging. *AJR Am J Roentgenol* 2005;185:1214-20.
- [30] Tempany CM, Zhou X, Zerhouni EA, et al. Staging of prostate cancer: results of Radiology Diagnostic Oncology Group project comparison of three MR imaging techniques. *Radiology* 1994;192:47-54.
- [31] Huch Boni RA, Boner JA, Lutolf UM, Trinkler F, Pestalozzi DM, Krestin GP. Contrast-enhanced endorectal coil MRI in local staging of prostate carcinoma. *J Comput Assist Tomogr* 1995;19:232-7.
- [32] Yu KK, Hricak H, Alagappan R, Chernoff DM, Bacchetti P, Zaloudek CJ. Detection of extracapsular extension of prostate carcinoma with endorectal and phased-array coil MR imaging: multivariate feature analysis. *Radiology* 1997;202:697-702.
- [33] Ikonen S, Karkkainen P, Kivisaari L, et al. Endorectal magnetic resonance imaging of prostatic cancer: comparison between fat-suppressed T2-weighted fast spin echo and three-dimensional dual-echo, steady-state sequences. *Eur Radiol* 2001;11:236-41.
- [34] Sala E, Akin O, Moskowitz CS, et al. Endorectal MR imaging in the evaluation of seminal vesicle invasion: diagnostic accuracy and multivariate feature analysis. *Radiology* 2006;238:929-37.
- [35] Park BK, Kim B, Kim CK, Lee HM, Kwon GY. Comparison of phased-array 3.0-T and endorectal 1.5-T magnetic resonance imaging in the evaluation of local staging accuracy for prostate cancer. *J Comput Assist Tomogr* 2007;31:534-8.
- [36] Casciani E, Polettini E, Bertini L, et al. Contribution of the MR spectroscopic imaging in the diagnosis of prostate cancer in the peripheral zone. *Abdom Imaging* 2007;32:796-802.
- [37] Cirillo S, Petracchini M, Della Monica P, et al. Value of endorectal MRI and MRS in patients with elevated prostate-specific antigen levels and previous negative biopsies to localize peripheral zone tumours. *Clin Radiol* 2008;63:871-9.
- [38] Tamada T, Sone T, Jo Y, et al. Prostate cancer: relationships between postbiopsy hemorrhage and tumor detectability at MR diagnosis. *Radiology* 2008;248:531-9.
- [39] Costouros NG, Coakley FV, Westphalen AC, et al. Diagnosis of prostate cancer in patients with an elevated prostate-specific antigen level: role of endorectal MRI and MR spectroscopic imaging. *AJR Am J Roentgenol* 2007;188:812-6.
- [40] Tanimoto A, Nakashima J, Kohno H, Shinmoto H, Kuribayashi S. Prostate cancer screening: the clinical value of diffusion-weighted imaging and dynamic MR imaging in combination with T2-weighted imaging. *J Magn Reson Imaging* 2007;25:146-52.
- [41] Chen M, Dang HD, Wang JY, et al. Prostate cancer detection: comparison of T2-weighted imaging, diffusion-weighted imaging, proton magnetic resonance spectroscopic imaging, and the three techniques combined. *Acta Radiol* 2008;49:602-10.
- [42] Kubota Y, Kamei S, Nakano M, Ehara H, Deguchi T, Tanaka O. The potential role of prebiopsy magnetic resonance imaging combined with prostate-specific antigen density in the detection of prostate cancer. *Int J Urol* 2008;15:322-6, discussion 327.
- [43] Coakley FV, Kurhanewicz J, Lu Y, et al. Prostate cancer tumor volume: measurement with endorectal MR and MR spectroscopic imaging. *Radiology* 2002;223:91-7.
- [44] Jager GJ, Ruijter ET, van de Kaa CA, et al. Local staging of prostate cancer with endorectal MR imaging: correlation with histopathology. *AJR Am J Roentgenol* 1996;166:845-52.

- [45] Yu KK, Scheidler J, Hricak H, et al. Prostate cancer: prediction of extracapsular extension with endorectal MR imaging and three-dimensional proton MR spectroscopic imaging. *Radiology* 1999;213:481–8.
- [46] Swanson MG, Vigneron DB, Tabatabai ZL, et al. Proton HR-MAS spectroscopy and quantitative pathologic analysis of MRI/3D-MRSI-targeted postsurgical prostate tissues. *Magn Reson Med* 2003;50:944–54.
- [47] Wefer AE, Hricak H, Vigneron DB, et al. Sextant localization of prostate cancer: comparison of sextant biopsy, magnetic resonance imaging and magnetic resonance spectroscopic imaging with step section histology. *J Urol* 2000;164:400–4.
- [48] Fütterer JJ, Scheenen TW, Heijmink SW, et al. Standardized threshold approach using three-dimensional proton magnetic resonance spectroscopic imaging in prostate cancer localization of the entire prostate. *Invest Radiol* 2007;42:116–22.
- [49] Manenti G, Squillaci E, Carlini M, Mancino S, Di Roma M, Simonetti G. Magnetic resonance imaging of the prostate with spectroscopic imaging using a surface coil. Initial clinical experience. *Radiol Med (Torino)* 2006;111:22–32.
- [50] Reinsberg SA, Payne GS, Riches SF, et al. Combined use of diffusion-weighted MRI and 1H MR spectroscopy to increase accuracy in prostate cancer detection. *AJR Am J Roentgenol* 2007;188:91–8.
- [51] Shimofusa R, Fujimoto H, Akamata H, et al. Diffusion-weighted imaging of prostate cancer. *J Comput Assist Tomogr* 2005;29:149–53.
- [52] DeSouza NM, Reinsberg SA, Scurr ED, Brewster JM, Payne GS. Magnetic resonance imaging in prostate cancer: the value of apparent diffusion coefficients for identifying malignant nodules. *Br J Radiol* 2007;80:90–5.
- [53] Morgan VA, Kyriazi S, Ashley SE, deSouza NM. Evaluation of the potential of diffusion-weighted imaging in prostate cancer detection. *Acta Radiol* 2007;48:695–703.
- [54] Yoshimitsu K, Kiyoshima K, Irie H, et al. Usefulness of apparent diffusion coefficient map in diagnosing prostate carcinoma: correlation with stepwise histopathology. *J Magn Reson Imaging* 2008;27:132–9.
- [55] Van As N, Charles-Edwards E, Jackson A, et al. Correlation of diffusion-weighted MRI with whole mount radical prostatectomy specimens. *Br J Radiol* 2008;81:456–62.
- [56] Jager GJ, Ruijter ET, van de Kaa CA, et al. Dynamic TurboFLASH subtraction technique for contrast-enhanced MR imaging of the prostate: correlation with histopathologic results. *Radiology* 1997;203:645–52.
- [57] Ogura K, Maekawa S, Okubo K, et al. Dynamic endorectal magnetic resonance imaging for local staging and detection of neurovascular bundle involvement of prostate cancer: correlation with histopathologic results. *Urology* 2001;57:721–6.
- [58] Kiessling F, Lichy M, Grobholz R, et al. Simple models improve the discrimination of prostate cancers from the peripheral gland by T1-weighted dynamic MRI. *Eur Radiol* 2004;14:1793–801.
- [59] Schlemmer HP, Merkle J, Grobholz R, et al. Can pre-operative contrast-enhanced dynamic MR imaging for prostate cancer predict microvessel density in prostatectomy specimens? *Eur Radiol* 2004;14:309–17.
- [60] Kim JK, Hong SS, Choi YJ, et al. Wash-in rate on the basis of dynamic contrast-enhanced MRI: usefulness for prostate cancer detection and localization. *J Magn Reson Imaging* 2005;22:639–46.
- [61] Fütterer JJ, Heijmink SW, Scheenen TW, et al. Prostate cancer localization with dynamic contrast-enhanced MR imaging and proton MR spectroscopic imaging. *Radiology* 2006;241:449–58.
- [62] Bloch BN, Furman-Haran E, Helbich TH, et al. Prostate cancer: accurate determination of extracapsular extension with high-spatial-resolution dynamic contrast-enhanced and T2-weighted MR imaging—initial results. *Radiology* 2007;245:176–85.
- [63] Ren J, Huan Y, Wang H, et al. Dynamic contrast-enhanced MRI of benign prostatic hyperplasia and prostatic carcinoma: correlation with angiogenesis. *Clin Radiol* 2008;63:153–9.
- [64] Kozlowski P, Chang SD, Jones EC, Berean KW, Chen H, Goldenberg SL. Combined diffusion-weighted and dynamic contrast-enhanced MRI for prostate cancer diagnosis—correlation with biopsy and histopathology. *J Magn Reson Imaging* 2006;24:108–13.
- [65] Mazaheri Y, Shukla-Dave A, Hricak H, et al. Prostate cancer: identification with combined diffusion-weighted MR imaging and 3D 1H MR spectroscopic imaging—correlation with pathologic findings. *Radiology* 2008;246:480–8.
- [66] Beyersdorff D, Taupitz M, Winkelmann B, et al. Patients with a history of elevated prostate-specific antigen levels and negative transrectal US-guided quadrant or sextant biopsy results: value of MR imaging. *Radiology* 2002;224:701–6.
- [67] Comet-Battle J, Vilanova-Busquets JC, Saladié-Roig JM, Gelabert-Mas A, Barceló-Vidal C. The value of endorectal MRI in the early diagnosis of prostate cancer. *Eur Urol* 2003;44:201–8, discussion 207–8.
- [68] Yuen JS, Thng CH, Tan PH, et al. Endorectal magnetic resonance imaging and spectroscopy for the detection of tumor foci in men with prior negative transrectal ultrasound prostate biopsy. *J Urol* 2004;171:1482–6.
- [69] Amsellem-Ouazana D, Younes P, Conquy S, et al. Negative prostatic biopsies in patients with a high risk of prostate cancer. Is the combination of endorectal MRI and magnetic resonance spectroscopy imaging (MRSI) a useful tool? A preliminary study. *Eur Urol* 2005;47:582–6.
- [70] Lattouf JB, Grubb 3rd RL, Lee SJ, et al. Magnetic resonance imaging-directed transrectal ultrasonography-guided biopsies in patients at risk of prostate cancer. *BJU Int* 2007;99:1041–6.
- [71] Silverman JM, Krebs TL. MR imaging evaluation with a transrectal surface coil of local recurrence of prostatic cancer in men who have undergone radical prostatectomy. *AJR Am J Roentgenol* 1997;168:379–85.
- [72] Sella T, Schwartz LH, Hricak H. Retained seminal vesicles after radical prostatectomy: frequency, MRI characteristics, and clinical relevance. *AJR Am J Roentgenol* 2006;186:539–46.

- [73] Casciani E, Poletini E, Carmenini E, et al. Endorectal and dynamic contrast-enhanced MRI for detection of local recurrence after radical prostatectomy. *AJR Am J Roentgenol* 2008;190:1187-92.
- [74] Sciarra A, Panebianco V, Salciccia S, et al. Role of dynamic contrast-enhanced magnetic resonance (MR) imaging and proton MR spectroscopic imaging in the detection of local recurrence after radical prostatectomy for prostate cancer. *Eur Urol* 2008;54:589-600.
- [75] Pucar D, Shukla-Dave A, Hricak H, et al. Prostate cancer: correlation of MR imaging and MR spectroscopy with pathologic findings after radiation therapy: initial experience. *Radiology* 2005;236:545-53.
- [76] Coakley FV, Teh HS, Qayyum A, et al. Endorectal MR imaging and MR spectroscopic imaging for locally recurrent prostate cancer after external beam radiation therapy: preliminary experience. *Radiology* 2004;233:441-8.
- [77] Zakian KL, Sircar K, Hricak H, et al. Correlation of proton MR spectroscopic imaging with Gleason score based on step-section pathologic analysis after radical prostatectomy. *Radiology* 2005;234:804-14.
- [78] Hom JJ, Coakley FV, Simko JP, et al. High-grade prostatic intraepithelial neoplasia in patients with prostate cancer: MR and MR spectroscopic imaging features—initial experience. *Radiology* 2007;242:483-9.
- [79] Padhani AR. Dynamic contrast-enhanced MRI in clinical oncology: current status and future directions. *J Magn Reson Imaging* 2002;16:407-22.
- [80] Engelbrecht MR, Huisman HJ, Laheij RJ, et al. Discrimination of prostate cancer from normal peripheral zone and central gland tissue by using dynamic contrast-enhanced MR imaging. *Radiology* 2003;229:248-54.
- [81] Padhani AR, Gapinski CJ, Macvicar DA, et al. Dynamic contrast enhanced MRI of prostate cancer: correlation with morphology and tumour stage, histological grade and PSA. *Clin Radiol* 2000;55:99-109.
- [82] Alonzi R, Padhani AR, Allen C. Dynamic contrast enhanced MRI in prostate cancer. *Eur J Radiol* 2007;63:335-50.
- [83] Shukla-Dave A, Hricak H, Kattan MW, et al. The utility of magnetic resonance imaging and spectroscopy for predicting insignificant prostate cancer: an initial analysis. *BJU Int* 2007;99:786-93.
- [84] Cookson MS, Fleshner NE, Soloway SM, Fair WR. Correlation between Gleason score of needle biopsy and radical prostatectomy specimen: accuracy and clinical implications. *J Urol* 1997;157:559-62.
- [85] Pondman KM, Fütterer JJ, ten Haken B, et al. MR-guided biopsy of the prostate: an overview of techniques and a systematic review. *Eur Urol* 2008;54:517-27.
- [86] Shukla-Dave A, Hricak H, Eberhardt SC, et al. Chronic prostatitis: MR imaging and 1H MR spectroscopic imaging findings—initial observations. *Radiology* 2004;231:717-24.

Embracing Excellence in Prostate, Bladder and Kidney Cancer

27-29 November 2009

Barcelona, Spain



www.emucbarcelona2009.org

2nd European Multidisciplinary Meeting on Urological Cancers organised by:

